Reduction of timing jitter and intensity noise in normal-dispersion passively mode-locked fiber lasers by narrow band-pass filtering

Peng Qin,[1] Youjian Song,[1,3] Hyoji Kim,[2] Junho Shin,[2] Dohyeon Kwon,[2] Minglie Hu,[1] Chingyue Wang,[1] and Jungwon Kim[2,*]

[1]*Ultrafast Laser Laboratory, Key Laboratory of Opto-electronic Information Technical Science of Ministry of Education, School of Precision Instruments and Opto-electronics Engineering, Tianjin University, Tianjin 300072, China*
[2]*School of Mechanical, Aerospace and Systems Engineering, Korea Advanced Institute of Science and Technology (KAIST), Daejeon 305-701, South Korea*
[3]*yjsong@tju.edu.cn*
[*]*jungwon.kim@kaist.ac.kr*

Abstract: Fiber lasers mode-locked with normal cavity dispersion have recently attracted great attention due to large output pulse energy and femtosecond pulse duration. Here we accurately characterized the timing jitter of normal-dispersion fiber lasers using a balanced cross-correlation method. The timing jitter characterization experiments show that the timing jitter of normal-dispersion mode-locked fiber lasers can be significantly reduced by using narrow band-pass filtering (e.g., 7-nm bandwidth filtering in this work). We further identify that the timing jitter of the fiber laser is confined in a limited range, which is almost independent of cavity dispersion map due to the amplifier-similariton formation by insertion of the narrow bandpass filter. The lowest observed timing jitter reaches 0.57 fs (rms) integrated from 10 kHz to 10 MHz Fourier frequency. The rms relative intensity noise (RIN) is also reduced from 0.37% to 0.02% (integrated from 1 kHz to 5 MHz Fourier frequency) by the insertion of narrow band-pass filter.

References and links

1. H. A. Haus and A. Mecozzi, "Noise of mode-locked lasers," IEEE J. Quantum Electron. **29**(3), 983–996 (1993).
2. R. Paschotta, "Noise of mode-locked lasers (Part II): timing jitter and other fluctuations," Appl. Phys. B **79**(2), 163–173 (2004).
3. N. R. Newbury, "Searching for applications with a fine-tooth comb," Nat. Photonics **5**(4), 186–188 (2011).
4. S. T. Cundiff and J. Ye, "Colloquium: femtosecond optical frequency combs," Rev. Mod. Phys. **75**(1), 325–342 (2003).
5. J. Kim, J. A. Cox, J. Chen, and F. X. Kärtner, "Drift-free femtosecond timing synchronization of remote optical and microwave sources," Nat. Photonics **2**(12), 733–736 (2008).
6. T. R. Schibli, J. Kim, O. Kuzucu, J. T. Gopinath, S. N. Tandon, G. S. Petrich, L. A. Kolodziejski, J. G. Fujimoto, E. P. Ippen, and F. X. Kaertner, "Attosecond active synchronization of passively mode-locked lasers by balanced cross correlation," Opt. Lett. **28**(11), 947–949 (2003).
7. J. Kim, J. Chen, J. Cox, and F. X. Kärtner, "Attosecond-resolution timing jitter characterization of free-running mode-locked lasers," Opt. Lett. **32**(24), 3519–3521 (2007).
8. Y. Song, K. Jung, and J. Kim, "Impact of pulse dynamics on timing jitter in mode-locked fiber lasers," Opt. Lett. **36**(10), 1761–1763 (2011).
9. A. J. Benedick, J. G. Fujimoto, and F. X. Kärtner, "Optical flywheels with attosecond jitter," Nat. Photonics **6**(2), 97–100 (2012).
10. P. T. Callahan, K. Safak, P. Battle, T. D. Roberts, and F. X. Kärtner, "Fiber-coupled balanced optical cross-correlator using PPKTP waveguides," Opt. Express **22**(8), 9749–9758 (2014).
11. Y. Song, C. Kim, K. Jung, H. Kim, and J. Kim, "Timing jitter optimization of mode-locked Yb-fiber lasers toward the attosecond regime," Opt. Express **19**(15), 14518–14525 (2011).

12. C. Kim, S. Bae, K. Kieu, and J. Kim, "Sub-femtosecond timing jitter, all-fiber, CNT-mode-locked Er-laser at telecom wavelength," Opt. Express **21**(22), 26533–26541 (2013).
13. J. P. Gordon and H. A. Haus, "Random walk of coherently amplified solitons in optical fiber transmission," Opt. Lett. **11**(10), 665–667 (1986).
14. F. Ö. Ilday, J. R. Buckley, W. G. Clark, and F. W. Wise, "Self-similar evolution of parabolic pulses in a laser," Phys. Rev. Lett. **92**(21), 213902 (2004).
15. B. Oktem, C. Ülgüdür, and F. Ömer Ilday, "Soliton–similariton fibre laser," Nat. Photonics **4**(5), 307–311 (2010).
16. W. H. Renninger, A. Chong, and F. W. Wise, "Pulse shaping and evolution in normal-dispersion mode-locked fiber lasers," IEEE J. Sel. Top. Quantum Electron. **18**(1), 389–398 (2012).
17. M. Baumgartl, C. Lecaplain, A. Hideur, J. Limpert, and A. Tünnermann, "66 W average power from a microjoule-class sub-100 fs fiber oscillator," Opt. Lett. **37**(10), 1640–1642 (2012).
18. C. Li, G. Z. Wang, T. X. Jiang, P. Li, A. M. Wang, and Z. Zhang, "Femtosecond amplifier similariton Yb:fiber laser at a 616 MHz repetition rate," Opt. Lett. **39**(7), 1831–1833 (2014).
19. A. Chong, H. Liu, B. Nie, B. G. Bale, S. Wabnitz, W. H. Renninger, M. Dantus, and F. W. Wise, "Pulse generation without gain-bandwidth limitation in a laser with self-similar evolution," Opt. Express **20**(13), 14213–14220 (2012), http://www.opticsinfobase.org/oe/abstract.cfm?uri=oe-20-13-14213.
20. N. B. Chichkov, C. Hapke, J. Neumann, D. Kracht, D. Wandt, and U. Morgner, "Pulse duration and energy scaling of femtosecond all-normal dispersion fiber oscillators," Opt. Express **20**(4), 3844–3852 (2012).
21. J. Lim, H.-W. Chen, G. Chang, and F. X. Kärtner, "Frequency comb based on a narrowband Yb-fiber oscillator: pre-chirp management for self-referenced carrier envelope offset frequency stabilization," Opt. Express **21**(4), 4531–4538 (2013), http://www.opticsinfobase.org/oe/abstract.cfm?uri=oe-21-4-4531.
22. L. A. Jiang, M. E. Grein, E. P. Ippen, C. McNeilage, J. Searls, and H. Yokoyama, "Quantum-limited noise performance of a mode-locked laser diode," Opt. Lett. **27**(1), 49–51 (2002).
23. C. Ouyang, P. Shum, H. Wang, J. H. Wong, K. Wu, S. Fu, R. Li, E. J. R. Kelleher, A. I. Chernov, and E. D. Obraztsova, "Observation of timing jitter reduction induced by spectral filtering in a fiber laser mode locked with a carbon nanotube-based saturable absorber," Opt. Lett. **35**(14), 2320–2322 (2010).
24. P. Li, W. Renninger, Z. Zhao, Z. Zhang, and F. Wise, "Frequency noise of amplifier-similariton laser combs," in *CLEO: 2013*, OSA Technical Digest (online) (Optical Society of America, 2013), paper CTu1I.6.
25. W. H. Renninger, A. Chong, and F. W. Wise, "Amplifier similaritons in a dispersion-mapped fiber laser [Invited]," Opt. Express **19**(23), 22496–22501 (2011), http://www.opticsinfobase.org/oe/abstract.cfm?uri=oe-19-23-22496.
26. I. L. Budunoğlu, C. Ulgüdür, B. Oktem, and F. Ö. Ilday, "Intensity noise of mode-locked fiber lasers," Opt. Lett. **34**(16), 2516–2518 (2009).
27. Y. Y. Zhang, C. Zhang, M. L. Hu, Y. J. Song, S. J. Wang, L. Chai, and C. Y. Wang, "High-energy subpicosecond pulse generation from a mode-locked Yb-doped large-mode-area photonic crystal fiber laser with fiber facet output," IEEE Photon. Technol. Lett. **22**(5), 350–352 (2010).

1. Introduction

Passively mode-locked lasers can generate optical pulse trains with extremely low timing jitter down to the attoseconds level, as predicted by laser noise theory [1,2]. Such a uniformly spaced pulse train has been proved to become an enabling signal source for a number of ultra-high precision applications, such as optical frequency metrology, low-noise microwave signal synthesis, arbitrary optical waveform generation, and large-scale timing distribution [3–5]. The direct observation of pulse train timing jitter from passively mode-locked lasers has also been enabled by a balanced optical cross-correlation (BOC) technique [6–10].

Compared to solid-state lasers, fiber lasers are more attractive for real-world applications due to their lower cost, more compact structure, and higher stability. Till now, all experimental demonstrations of timing jitter reduction in fiber lasers have required a careful optimization of cavity dispersion towards zero [11,12], where the pulse train is immune to the Gordon-Haus jitter [13]. However, fiber lasers working in the vicinity of zero dispersion often suffer from low pulse energy and multi-pulse instability. Normal dispersion fiber lasers have attracted much attention in recent years due to their advantage of large energy output, compact design and enhanced stability [14–18]. The compressed pulse duration already reaches the level of fiber lasers with close-to-zero cavity dispersion [19,20]. Optical frequency comb based on normal dispersion Yb-fiber lasers has also been demonstrated [21]. However, fiber lasers operating at normal dispersion is proved to have much larger jitter due to the larger Gordon-Haus jitter as has been experimentally characterized in [8]. It has been shown both theoretically [1,2] and experimentally [22,23] that intra-cavity filtering can act as a restoring force to reduce Gordon-Haus jitter in passively mode-locked lasers. It has been

also predicted that a narrow bandpass filter can make the jitter independent of cavity dispersion map due to amplifier-similariton formation [24].

In this paper, we study the timing jitter reduction effects in normal-dispersion fiber lasers using a BOC method. The timing jitter characterization experiments show that the timing jitter of normal-dispersion mode-locked fiber lasers can be significantly reduced by using narrow band-pass filtering (e.g., 7-nm bandwidth filtering in this work). Further, we could experimentally confirm that the resulting timing jitter is almost independent of cavity dispersion by the amplifier-similariton formation. As a result of suppressed Gordon-Haus jitter by narrow bandpass filtering, the observed timing jitter could be reduced to the sub-femtosecond regime (0.57 fs rms integrated from 10 kHz to 10 MHz Fourier frequency). We also find that the narrow band-pass filtering can result in much-reduced relative intensity noise (RIN), as observed by an amplitude noise characterization. The RIN reduction from 0.37% to 0.02% (in rms), integrated from 1 kHz to 5 MHz Fourier frequency, is observed by insertion of a narrow band-pass filter in the normal-dispersion passively mode-locked fiber lasers.

2. Experimental setup

The laser under test (LUT) is a standard nonlinear polarization evolution (NPE)-based mode-locked Yb-doped fiber laser, which is based on a ring cavity configuration, as shown in Fig. 1(a). A segment of 25 cm highly doped Yb-fiber is used as a gain medium. The pump is provided by a 660-mW fiber-Bragg-grating stabilized low intensity noise telecom laser diode working at 976 nm. The total intra-cavity fiber length is 80 cm, and the cavity normal dispersion is ~0.02 ps^2. A 600 grooves/mm grating pair is used for dispersion compensation. The net cavity dispersion can be tuned continuously by altering the grating pair separation. The laser repetition rate is fixed at 161 MHz by adjusting the free space optical path at different grating pair separation. In order to study the impact of spectral filtering on timing jitter of the normal dispersion mode-locked fiber laser, an interferometric band-pass filter with 7 nm 3-dB bandwidth centered at 1040 nm is inserted after the isolator in the LUT.

Several mode-locking conditions are found by altering the dispersion map and spectral filtering under the normal intra-cavity dispersion. The optical spectra of the laser output at these mode-locking conditions are presented in Fig. 1(b). The laser works in a passive self-similar regime at a cavity dispersion of ~0.004 ps^2 and ~0.008 ps^2. When the narrow band-pass filter is inserted into the cavity, the pulse dynamics converts to an amplifier-similariton formation in dispersion mapped fiber lasers [25], despite the large difference in cavity dispersion. The grating pair can be also removed, resulting in an all-normal-dispersion (ANDi) mode-locked fiber laser operating at ~0.02 ps^2. Note that, at + 0.02 ps^2 condition, the ultrashort pulse operation can be stabilized only when the spectral filter is inserted.
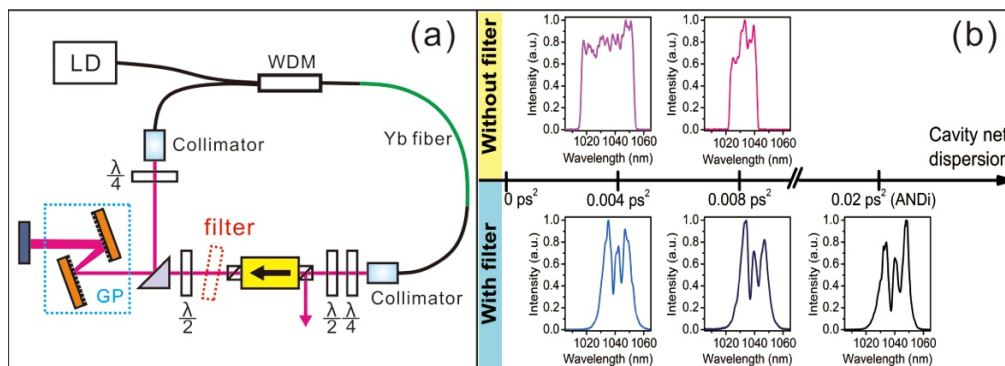

Fig. 1. (a) Configuration of the passively mode-locked Yb-fiber laser under test. GP, grating pair; LD, 976-nm laser diode; WDM, wavelength division multiplexer; (b) Laser output spectra at normal dispersion regime with different cavity dispersion in the presence or absence of a narrow band-pass filter.

The timing jitter of the passively mode-locked fiber lasers with various operation modes is characterized by the BOC between the LUT and an independent reference laser (REF). The setup of timing jitter characterization is shown in Fig. 2. The REF is based on a σ-cavity design with a piezoelectric transducer (PZT)-mounted mirror, which is used for repetition rate locking between the two lasers. The reference laser is a standard Yb-doped stretched-pulse fiber laser working in the vicinity of zero cavity dispersion, which characterizes an ultralow timing jitter of 270 as timing jitter [integrated from 10 kHz to 10 MHz offset frequency].
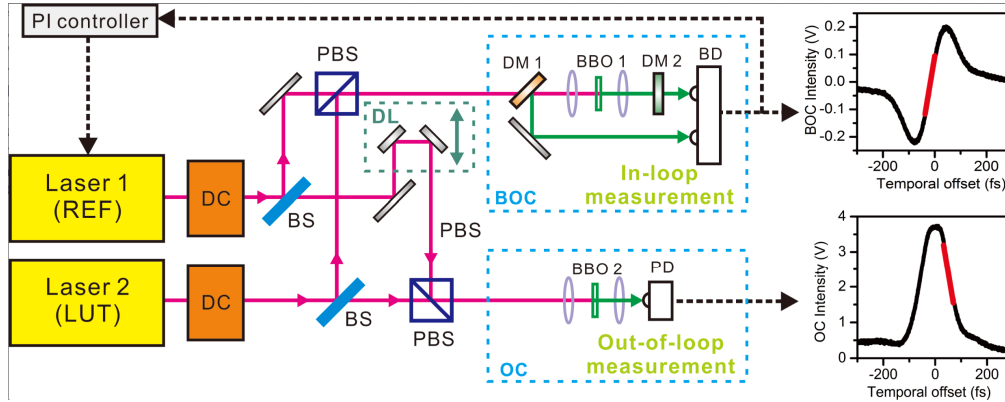

Fig. 2. Configuration of the timing jitter characterization system. BBO, beta-barium borate; BD, Balanced photo-detector; BS, 50:50 beam splitter; BOC, balanced optical cross-correlator; DC, dispersion compensation; DL, delay line; DM, dichroic mirror; OC, optical cross-correlator; PBS, polarization beam splitter; PD, photo-detector. Inset: The error voltage signal from the BOC and OC output.

The output pulses from the two lasers are extra-cavity dechirped, combined by a polarization beam splitter (PBS), and directed to the BOC. The configuration of BOC is shown in Fig. 2. The cross correlation is realized by focusing the two pulse trains with orthogonal polarization states into a 650-μm thick, type-II phase-matched beta-barium borate (BBO) crystal for sum-frequency generation (SFG). The intensity of the SFG signal is related to the relative timing between the pulse trains. In order to remove the SFG contribution that is originated from the intensity fluctuation of the input pulse trains, the pulse trains after transmission from BBO are reflected back by a dichroic mirror (DM 2 in Fig. 2) for another identical SFG. The transmitted SFG signals are detected by a high-speed balanced photodetector (Newfocus, Model 1807) with a cutoff frequency of ~60 MHz. The resulting BOC output is shown in the inset of Fig. 2. The linear range of the voltage signal is proportional to the relative timing jitter between the two lasers, providing a timing error discriminator that can be received by a radio-frequency (RF) spectral analyzer, which characterizes the timing jitter spectral density of two independent lasers. The measured result gives an upper estimate for the timing jitter of the LUT assuming a negligible timing jitter contribution from REF.

The dynamic range of the BOC is limited within the linear range of the error voltage signal. Therefore, we phase-lock the repetition rate of the two lasers with a locking bandwidth of ~3 kHz. The residual in-loop (IL) timing jitter is characterized outside the locking bandwidth. After the tight repetition rate locking is achieved by the in-loop BOC, an independent out-of-loop (OOL) single-pass optical cross-correlator is used in order to check the validity of the in-loop timing jitter characterization. The single pass cross-correlation is based on SFG in a piece of type-II phase-matched BBO with 450-μm thickness. The cross-correlation trace is shown in the inset of Fig. 2. The OOL timing jitter is recorded when the two pulses are offset by ~1/2 pulse duration, where the largest timing jitter to voltage discrimination is achieved.

3. Experimental results

The timing jitter of the five LUT operation modes in Fig. 1(b) with different amount of normal cavity dispersion in the presence or in the absence of narrow band-pass filter is characterized. At each dispersion point with given filtering condition, stable mode-locking is achieved by simple adjustment of waveplate settings.

The laser output parameters for different mode-locking conditions are summarized in Table 1. The pump power for each laser operation mode is set to the same level for each mode-locking condition except for the ANDi cavity, which shows a higher mode-locking threshold. The output average power ranges from 120 mW to 200 mW. The slight difference of laser output power at the same pump power is due to the difference in output coupling ratio introduced by NPE. The direct output pulse duration will decrease with cavity dispersion in the absence of narrow band-pass filtering. However, when the filter is inserted into the cavity, the laser shows similar direct output pulse duration regardless of cavity dispersion. The dechirped pulse duration for all the five mode-locking conditions lies in a similar level.

Table 1. Laser output parameters for different mode-locking conditions

	0.004 ps^2		0.008 ps^2		0.02 ps^2
	PSS [a]	*AS* [b]	*PSS*	*AS*	*ANDi* [c]
Pump power (W)	0.4	0.4	0.4	0.4	0.52
Output power (W)	0.14	0.13	0.16	0.12	0.2
Direct output pulse duration (ps)	1.23	0.56	2.3	0.54	0.75
Dechirped pulse duration (ps)	0.12	0.11	0.16	0.11	0.11

[a] PSS, Passive self-similar; [b] AS, Amplifier similariton; [c] ANDi, All normal dispersion.

First, the timing jitter of the Yb-fiber laser under ANDi mode-locking is characterized. The IL and OOL jitter spectral density is characterized by BOC and OC methods, respectively, which are shown in Fig. 3(a). Beyond locking bandwidth, both of the jitter spectra basically follow a characteristic −20 dB/decade slope from 10 kHz to 10 MHz, which indicates a random walk of pulse train timing jitter directly coupled from the white noise of the ASE in the gain fiber. The IL and OOL jitter spectra overlap very well above 100 Hz Fourier frequency, which confirms the validity of the IL jitter measurement based on the BOC method. The in-loop jitter spectrum above 10 MHz Fourier frequency is limited by the photodetector sensitivity. When integrated from 10 kHz to 10 MHz Fourier frequency, the residual rms timing jitter of the ANDi laser is 1.09 fs.

The relative intensity noise (RIN) of the ANDi laser is also characterized. The RIN measurement is based on a standard direct photo-detection method. The RIN of mode-locked fiber laser in different dispersion map from large negative dispersion to normal dispersion has been discussed in an earlier publication [26]. The reduction of RIN by filtering has also been demonstrated in soliton and soliton-similariton regime [15, 27]. Here, we focus on the impact of narrow spectral filtering on the RIN in normal dispersion mode-locked fiber lasers. A fraction of laser output is directed to a high-speed, low-noise amplified photo-detector (Thorlabs, FPD510). A 0.5 mW of optical power is used before the saturation of the photo-detector. Then, the photo-detected error signal passes through a low pass filter with 10 MHz cutoff frequency. After low pass filtering, the low frequency (DC-100 kHz) and the high frequency (>100 kHz) parts of the error voltage are recorded by an FFT analyzer and an RF spectrum analyzer, respectively. The characterized RIN is shown in Fig. 3(b). The integrated rms RIN is 0.02% integrated from 1 kHz to 5 MHz in the ANDi laser. Note that the equivalent noise floor by the used photodetector is $\sim 10^{-17}$, which is much lower than the measured RIN level.
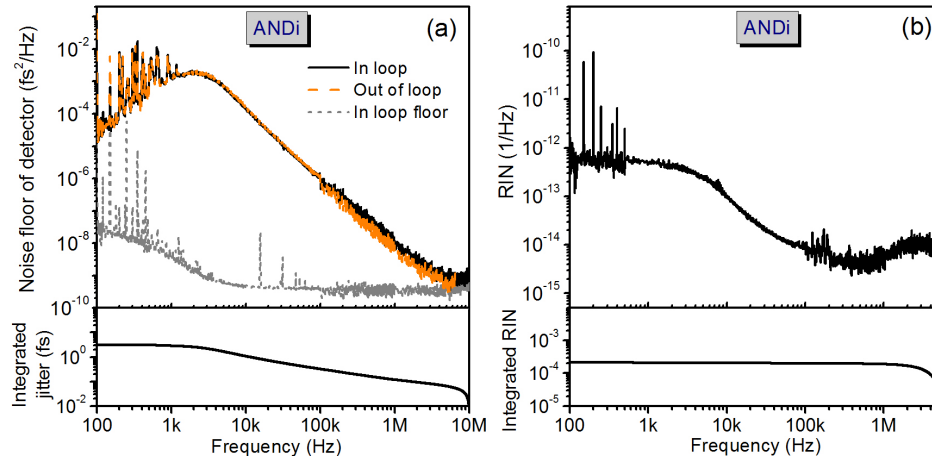
Fig. 3. Power spectral density of (a) timing jitter and (b) RIN of the ANDi laser operating at + 0.02 ps^2. The dashed line shows the electronic noise floor of the balanced detector for in-loop timing jitter characterization.

After characterizing the ANDi laser, by inserting a grating pair in the LUT, the timing jitter of the Yb-fiber laser with dispersion map is characterized. Passive mode-locking at two different cavity dispersion conditions (+ 0.008 ps^2 and + 0.004 ps^2) are studied. At each cavity dispersion, the timing jitter spectra with and without a 7-nm band-pass filter are characterized, which are shown in Fig. 4. The jitter spectrum of the ANDi laser (as shown in Fig. 3) is plotted in the same figure for ease of comparison. Figure 4(a) shows the jitter spectral density in the presence and in the absence of 7 nm filter at + 0.008 ps^2 cavity dispersion. By insertion of the narrow band-pass filter, more than 20 dB reduction of timing jitter power spectral density is observed, and the corresponding rms integrated jitter is reduced from 7.1 fs to 0.57 fs [10 kHz-10 MHz]. Figure 4(b) shows the jitter spectral density in the presence and in the absence of 7 nm filter at + 0.004 ps^2 cavity dispersion. By insertion of the narrow band-pass filter, ~10 dB reduction of timing jitter power spectral density is observed, and the corresponding rms integrated jitter is reduced from 2 fs to 0.92 fs [10 kHz-10 MHz].

As can be seen in Fig. 4(a) and Fig. 4(b), in the passive self-similar regimes without an intra-cavity filter, the timing jitter decreases when the cavity dispersion magnitude decreases towards zero. In this experiment, the jitter is reduced by >10 dB by decreasing the cavity dispersion from + 0.008 ps^2 to + 0.004 ps^2. There are two contributions for this jitter reduction. Firstly, the ASE-limited direct timing jitter is reduced due to the average pulse duration shortening inside the laser cavity by decreasing the cavity dispersion, which can be inferred from Table 1. Secondly, the Gordon-Haus jitter also reduces due to the decrease of net cavity dispersion.
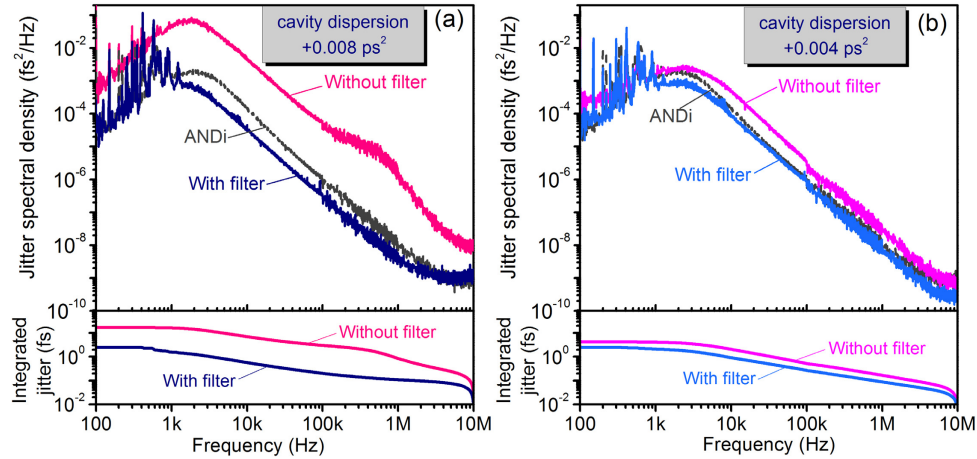
Fig. 4. The timing jitter spectra and the integrated jitter in the presence and in the absence of 7-nm filter at (a) + 0.008 ps^2 cavity dispersion and (b) + 0.004 ps^2 cavity dispersion. The jitter spectrum of the ANDi laser (from Fig. 3(a)) is plotted in the same figure for ease of comparison.

At each fixed cavity dispersion, we find that the timing jitter can be reduced by an intra-cavity narrow band-pass filter. Interestingly, by insertion of the filter, the jitter level becomes similar to the jitter from the ANDi laser, even at significantly different cavity dispersion, as shown in Fig. 4. This observation reflects the fact that the laser is changed from a passive self-similar mode-locking regime to an amplifier-similariton regime by including the intra-cavity narrow band-pass filter. The cavity dispersion plays a less role for pulse formation than the narrow band-pass filtering in an amplifier-similariton fiber laser, which can be confirmed from the optical spectra in Fig. 1(b).

As inferred from Table 1, the average pulse duration inside the cavity at different cavity dispersion is similar for the amplifier-similariton regime, which implies that these mode-locking conditions have similar quantum-limited timing jitter directly coupled from ASE. These mode-locking conditions are supposed to have very different jitter level due to the Gordon-Haus jitter (indirectly coupled from ASE-induced frequency noise through cavity dispersion). However, our observation shows a similar timing jitter level even at very different cavity dispersion. This indicates that Gordon-Haus jitter is significantly reduced by filtering effect.

The RIN of the Yb-fiber laser with dispersion map is also characterized. The measured RIN spectra and integrated RIN at + 0.008 ps^2 and + 0.004 ps^2 cavity dispersion are shown in Fig. 5. The RIN behaves similarly with timing jitter in the dispersion mapped fiber laser. In the passive self-similar regime without filtering, the RIN becomes higher at larger intra-cavity dispersion due to the weaker energy stabilization mechanism. In this experiment, the integrated RIN is reduced from 0.37% to 0.14%, integrated from 1 kHz to 5 MHz, by decreasing the cavity dispersion from + 0.008 ps^2 to + 0.004 ps^2. By insertion of the filter, the integrated RIN can be further decreased to 0.02% and 0.057% integrated from 1 kHz to 5 MHz, at cavity dispersion of + 0.008 ps^2 and + 0.004 ps^2, respectively. Since the amplifier similariton formation acts as a nonlinear attractor that stabilizes the mode-locking, the RIN (including the broad bump at ~500 kHz) is greatly suppressed by intra-cavity filtering as shown in Fig. 5(a). Also note that the RIN of dispersion-mapped fiber lasers with intra-cavity narrow band-pass filtering approaches to that of the ANDi laser, regardless of the cavity dispersion difference.
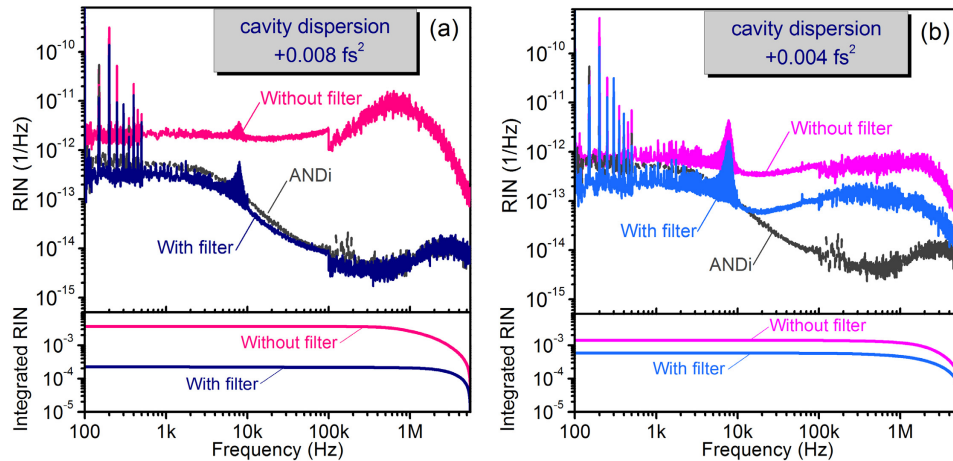
Fig. 5. The relative intensity noise (RIN) spectra and the integrated RIN in the presence and in the absence of 7-nm filter at (a) 0.008 ps^2 cavity dispersion and (b) 0.004 ps^2 cavity dispersion. The RIN of the ANDi laser is plotted in the same figure for ease of comparison.

4. Conclusion

In conclusion, the timing jitter of normal-dispersion fiber lasers is accurately characterized using an attosecond-resolution BOC method. Several mode-locking conditions are investigated in terms of cavity dispersion map and narrow band-pass filtering. The timing jitter of dispersion-mapped fiber lasers with intra-cavity narrow band-pass filtering approaches to that of the ANDi laser, despite the large difference in cavity dispersion. This interesting observation reflects the fact that the cavity dispersion plays a less role for pulse formation than the narrow band-pass filtering due to amplifier-similariton formation. As a result, similar timing jitter is observed at different cavity dispersion. The lowest observed timing jitter reaches 0.57 fs integrated from 10 kHz to 10 MHz Fourier frequency. The integrated rms RIN reduction from 0.37% to 0.02% (integrated from 1 kHz to 5 MHz) is also observed by insertion of the narrow band-pass filter. Particularly, much lower timing jitter and RIN in normal-dispersion fiber lasers can be simply achieved by a narrow band-pass filter. This results in a robust mode-locking operation, whereas the fine optimization of cavity dispersion for reduced Gordon-Haus jitter is not required any more. Such sub-fs jitter, low-RIN, narrow band-pass filter-stabilized fiber lasers show a great potential for more practical high-precision timing applications in the future.